



Non-innocent ligands for efficient dehydrogenation of aqueous and neat formic acid under base-free conditions

Liwei Guo, Zilong Li, Marie Cordier, Rémi Marchal, Boris Le Guennic, Cédric Fischmeister

► To cite this version:

Liwei Guo, Zilong Li, Marie Cordier, Rémi Marchal, Boris Le Guennic, et al.. Non-innocent ligands for efficient dehydrogenation of aqueous and neat formic acid under base-free conditions. *ACS Catalysis*, 2023, 13 (20), pp.13626-13637. 10.1021/acscatal.3c02060 . hal-04301582

HAL Id: hal-04301582

<https://univ-rennes.hal.science/hal-04301582v1>

Submitted on 23 Nov 2023

HAL is a multi-disciplinary open access archive for the deposit and dissemination of scientific research documents, whether they are published or not. The documents may come from teaching and research institutions in France or abroad, or from public or private research centers.

L'archive ouverte pluridisciplinaire **HAL**, est destinée au dépôt et à la diffusion de documents scientifiques de niveau recherche, publiés ou non, émanant des établissements d'enseignement et de recherche français ou étrangers, des laboratoires publics ou privés.

Non-innocent ligands for efficient dehydrogenation of aqueous and neat formic acid under base-free conditions

Liwei Guo, Zilong Li, Marie Cordier, Remi Marchal, Boris Le Guennic and Cédric

*Fischmeister**

Univ Rennes, CNRS, ISCR (Institut des Sciences Chimiques de Rennes) – UMR 6226

F-35042 Rennes, France. E-mail : cedric.fischmeister@univ-rennes.fr

KEYWORDS: Hydrogen; Liquid Organic Hydrogen Carriers; Formic acid; Homogeneous catalysis; iridium; metal-ligand cooperation; DFT

ABSTRACT : Formic acid could play an important role in the energy transition if robust catalysts for its efficient dehydrogenation are developed. Most importantly, additive-free protocols are sought to reduce the cost and simplify the dehydrogenation process. Ideally, the highest energy concentration requires the use of neat formic acid for which only a few catalysts, active under additive-free conditions, have been reported. We have prepared several new ruthenium and iridium

complexes incorporating dipyridylamine ligands with various electronic and steric properties. Among all these complexes, the air stable **Ir8** bearing a bis-dimethylamino-substituted dipyridylamine ligand displayed the best performances in the dehydrogenation of aqueous solutions of formic acid in the absence of any additives. The same catalyst could also dehydrogenate neat formic acid with a TOF of 11373 h⁻¹ at 80 °C. High H₂/CO₂ pressure, CO- free gas stream and catalyst latency enabling storage and further use of FA/catalyst premix have been achieved. Experimental and theoretical studies have highlighted the roles of dipyridylamine and SO₄ ligand in the dehydrogenation process.

INTRODUCTION

The inevitable decline of fossil resources has already begun and intense researches are underway to find alternative ways to feed both the energy supply chain and the chemical industry. There are several options for the transition to sustainable energy sources, such as hydro- and geothermal energy. Solar and wind energy are also at the forefront of sustainable energy, but they suffer from a major problem related to their intermittent nature and the inability to store large quantities of electricity. Osmotic energy has also seen important developments in the recent time.¹ Although its origins date back to the 1970s, hydrogen as an energy carrier has really taken off in the last 15 years. In his early introduction on hydrogen economy in 1972, Bockris proposed that the electricity carrier for future generations should not be electrons but hydrogen.² Indeed, hydrogen can be stored on large scale and used to generate electricity on demand using fuel-cells. Hydrogen, turns to be a versatile energy carrier, however, due to its dangerousness and gaseous nature, its storage and transportation suffers from some issues.³ Besides its utility in the energy sector, hydrogen also plays an important role in chemical reduction processes. These processes have been used for a

long time in many industrial processes, but they will undoubtedly increase significantly in the near future due to the transition from low-oxidation state fossil resources to high-oxidation state renewable resources as raw materials for the chemical industry.⁴

While the chemical industry's hydrogen supply chain is well established, the development of a hydrogen-based energy chain will certainly put the hydrogen sector under stress, creating the need for new hydrogen production, storage and transport routes. If water splitting⁵ using renewable energy seems to be the future direction for the production of “green hydrogen”,⁶ hydrogen storage and transportation is a complex issue to address due to the hazardous and gaseous nature of hydrogen.⁷ For these reasons, the storage of hydrogen in non-hazardous or low-hazard organic molecules has been attracting interest in the past two decades.⁸ Among these liquid organic hydrogen (LOHC) carriers, formic acid is considered, for several reasons, as one of the realistic options for hydrogen storage.⁹ First, formic acid which is currently essentially produced from fossil resources could also be produced in more sustainable fashions in a carbon neutral process by CO₂ hydrogenation using (captured) CO₂ and (green) hydrogen. However, CO₂ hydrogenation to formic acid is not at all a trivial reaction and other routes such as the transformation of lignocellulosic biomass are also in progress.¹⁰ Secondly, formic acid can be used to deliver hydrogen on demand for energy production, and it can also be directly engaged in chemical reduction processes as a hydrogen donor. This versatility makes formic acid one of the key compounds to meet the challenges of the energy and chemical transition. Homogeneous organometallic catalysts have been reported for the dehydrogenation of formic acid as well as for its use as a hydrogen donor in reduction processes. In both domains, basic additives have been used in the vast majority of cases in order to ensure catalytic turnovers.^{11,12} The stability of catalysts in acidic conditions is also a major issue to consider.

Recently, we have synthesized versatile ruthenium and iridium catalysts based on *N,N*-chelating dipyridylamine ligand¹³ which are able to perform the base-free reduction of levulinic acid, a biosourced platform chemical precursor for a number of chemicals,¹⁴ into γ -valerolactone (GVL)¹⁵ and *N*-heterocycles.¹⁶ The same catalysts also displayed high performances in the domain of Liquid Organic Hydrogen Carriers since some of them exhibited very high performances for the base-free dehydrogenation of aqueous solutions of formic acid and dehydrogenation of neat formic acid.^{17,18,19} In this article, we present our research on the synthesis of new iridium and ruthenium complexes with the aim of increasing the performance and elucidating the catalytic mechanism of the dehydrogenation of formic acid. Several new complexes featuring electron-rich ligands have been prepared and evaluated in the dehydrogenation of formic acid. In particular, a high TOF was obtained with an iridium catalyst in the dehydrogenation of aqueous and neat formic acid in the absence of any additive. Mechanistic investigations evidenced the crucial role of the SO_4^{2-} anion in the dehydrogenation process.

RESULTS AND DISCUSSION

Catalyst syntheses

A number of studies highlight the value of using electron-enriched metal complexes,²⁰ showing a strong correlation between the activity and hydricity of the catalysts.²¹ Numerous examples also highlight the crucial role of H-bond networks in the mechanism of catalytic dehydrogenation of formic acid.²² Based on these considerations, 3 families of dipyridylamine ligands were developed, one with electron-donating substituents, one with H-bond donor groups in the close vicinity of the metal centre and the last one with both an electron-donating substituent and a H-bond donor group. Steric effects were also investigated by preparing dipyridylamine ligands substituted at the 6-

position with methyl- and methoxy- substituents. The synthesis of all the dipyriddyamine ligands was performed using Pd-catalyzed amination reactions as illustrated in Figure 1 for the synthesis of the 4,4'-(dimethylamino)-2,2'-dipyriddyamine ligand **L4** (see ESI for full details of ligand syntheses including previously reported **L1** and **L2-L3**).

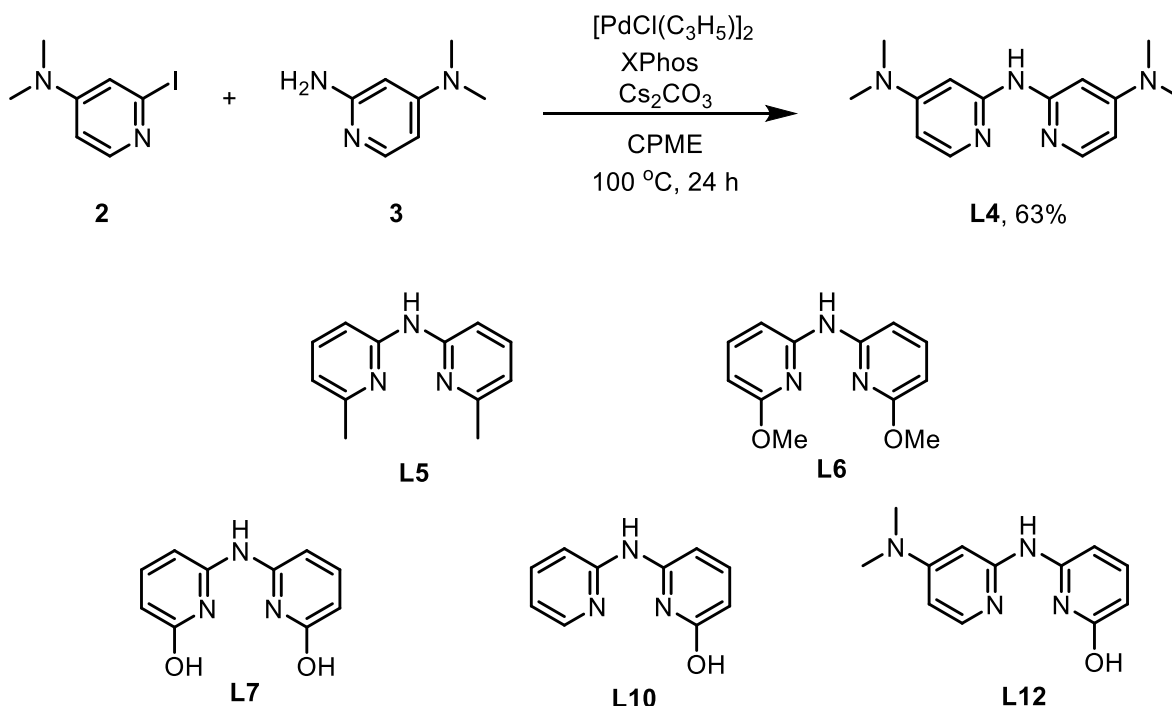


Figure 1 Synthesis of the 4,4'-(dimethylamino)-2,2'-dipyriddyamine ligand **L4**

Previous studies with $(\text{Ru}(\text{dipyriddyamine})(\eta^6\text{-}p\text{-cymene}))\text{OSO}_3$ catalyst **Ru1** (Figure 2) revealed the modest performances of this complex in formic acid dehydrogenation.¹⁵ The synthesis of electron rich complexes was then performed using Cp^* and dipyriddyamine ligands functionalized by electron donating dimethylamino-group, which are among the more electron-donating neutral organic substituents. The new complexes **Ru2-Ru5** were obtained as red powders in 81-87% yield (Figure 2).

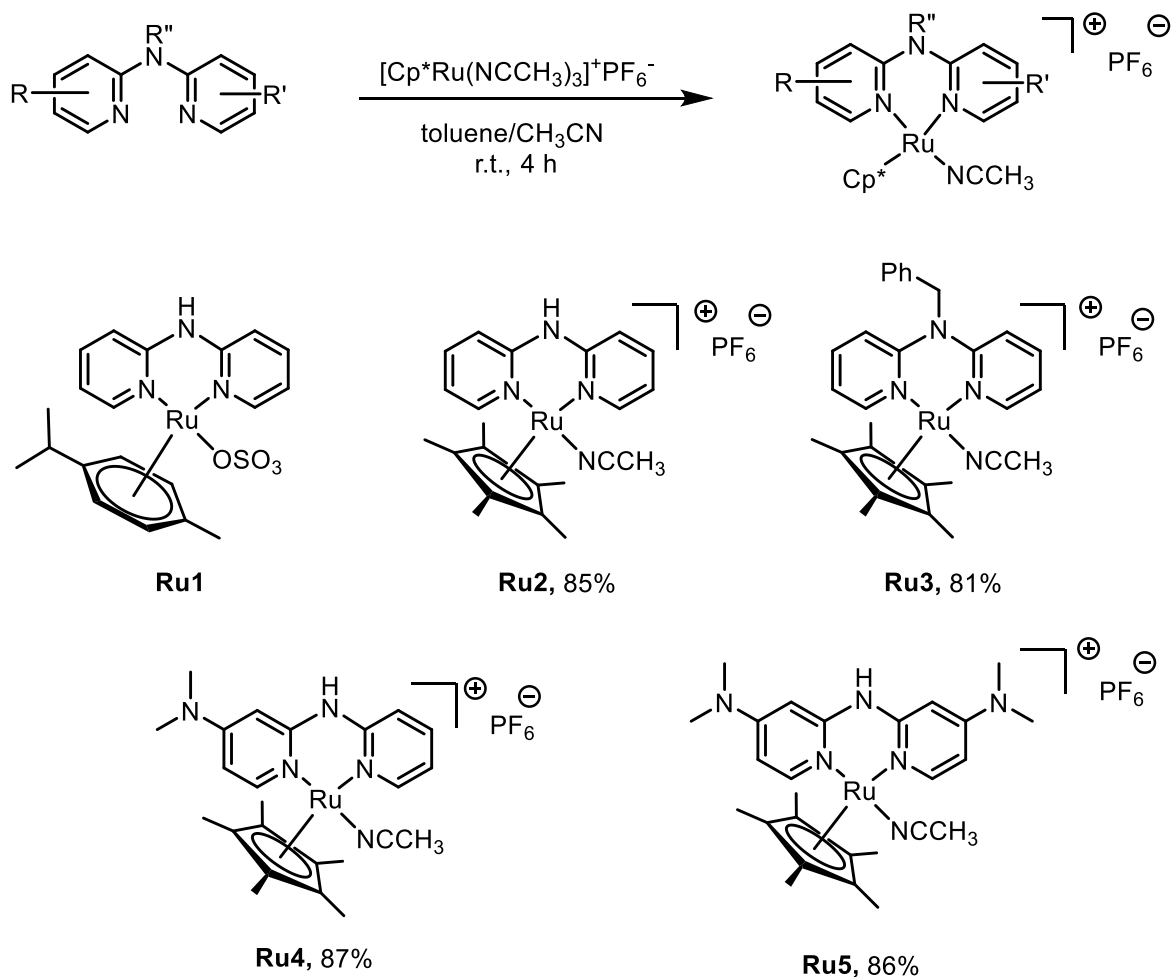


Figure 2 Ruthenium catalysts synthesis. (**Ru1** was previously reported^{15b})

Similarly, the new cationic iridium complexes **Ir2**, **Ir9**, **Ir10**, **Ir11** were prepared in good to excellent yields from $[\text{Cp}^*\text{IrCl}_2]_2$ (Figure 3). Abstraction of the chloride ligand provided the new zwitterionic complexes **Ir4**, **Ir5**, **Ir8**, **Ir12**, **Ir13**, **Ir14** also isolated in good to excellent yields. The zwitterionic nature of these complexes was assumed based on previous results^{15b} and confirmed hereafter for **Ir8**. It is worth mentioning that these 18-electron complexes are air stable and can be stored for weeks on the benchtop without strict exclusion of air.

Several complexes could be crystallized and their molecular structure determined by X-Ray diffraction. In particular, the molecular structures of **Ir2** and **Ir8** bearing the bis-4,4'-dimethylamino-dipyridylamine ligand were obtained, evidencing the zwitterionic nature of **Ir8** in the solid state (Figure 4).

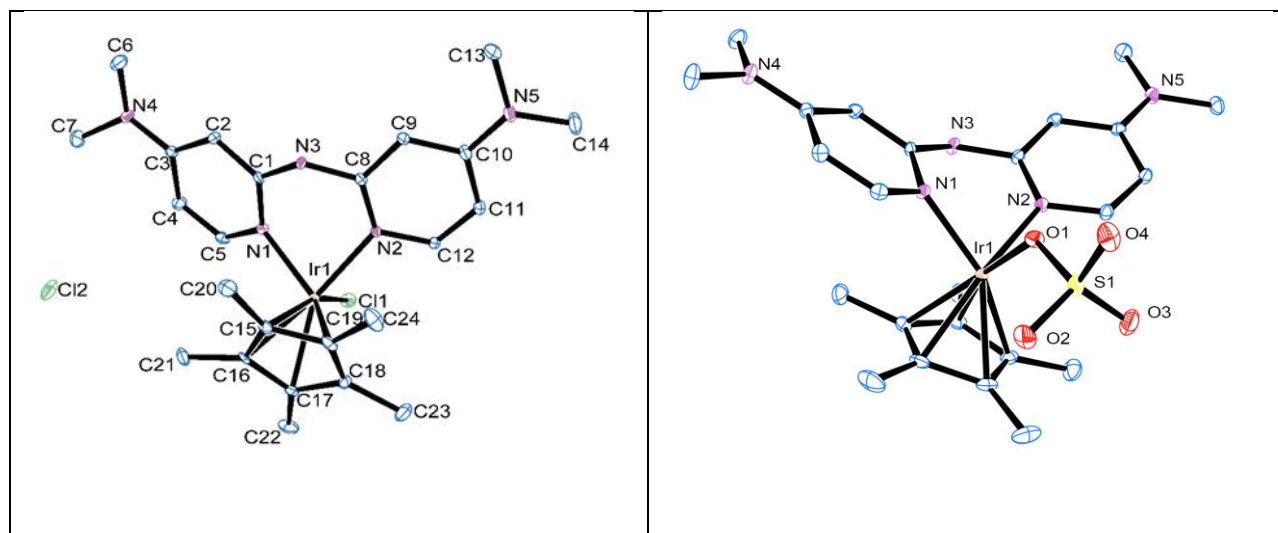
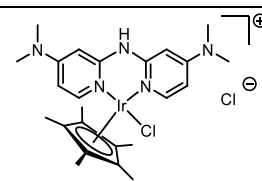
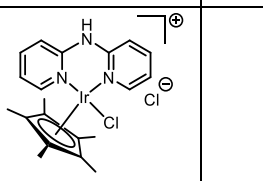
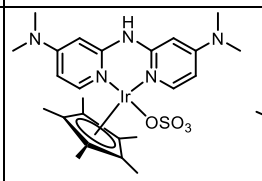
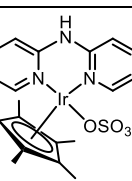


Figure 4 Molecular structures of **Ir2** (left) and **Ir8** (right). Ellipsoids are shown at 30% probability. H atoms are omitted for clarity.

Some structural parameters were gathered and compared between the already reported complexes **Ir1**, **Ir3** and the new complexes **Ir2**, **Ir8**. As depicted in Table 1, no major structural variations could be denoted between these complexes. Therefore, any variation of the catalytic performances within these catalysts should be attributed to electronic rather than steric influence. Finally, it is worth noting the planar geometry of the dimethylamino-substituent in **Ir8** (Σ bond angles around N4 & N5 = 360°) along with a short $C_{ar}-N$ bond length (1.35 Å) while the bridging amine was nearly planar (Σ bond angles around N3 = 353°) with $C_{ar}-N$ bond length of 1.40 Å).²³ These structural properties reflect the conjugation of the nitrogen electron pair with the phenyl rings.

They are also an indication of the weak basicity of this amino ligand having in mind that these complexes will be used in acidic media.

Table 1 selected bond lengths and bond angles for **Ir2**, **Ir8**, compare with **Ir1**, **Ir3**.^a

	Ir2	Ir1		Ir8	Ir3
					
Ir1-Cl1	2.405	2.38	Ir1-O1	2.094	2.101
Ir1-N1	2.089	2.094	Ir1-N1	2.090	2.104
Ir1-N2	2.093	2.102	Ir1-N2	2.087	2.096
Ir1-Cp* centroid ^b	1.779	1.778	Ir1-Cp* centroid ^b	1.783	1.786
N1Ir1N2	83.22	83.96	N1Ir1N2	83.01	84.06
Cl1Ir1N1	87.47	87.68	O1Ir1N1	80.39	79.63
Cl1Ir1N2	88.03	87.59	O1Ir1N2	79.52	82.73
C1N3C8	126.2	127.90	C1N3C8	125.5	125.1
PyN3Py ^c	152.1	153.55	PyN3Py ^c	147.2	146.5

^aBond lengths (Å), angles (deg). ^bCtd = Cp* centroid. ^cAverage plane calculated from pyridine rings and N3.

Complex **Ir11** bearing a doubly-modified dpa ligand was also characterized by X-Ray diffraction (Figure 5). As for the previously described complexes, we did not observe any major changes in the main structural data (see ESI), except for a slight lengthening of the Ir-N bond of the pyridine ring bearing the hydroxyl group due to increased steric hindrance (2.136 in **Ir11** vs 2.094 in **Ir1**).

Most importantly, a hydrogen bond was observed between the chloro-ligand and the hydroxyl group with a bond length of 2.21 Å (O-H...Cl) (Figure 5). This observation validates our initial hypothesis which consisted in bringing an H-bond donor that could participate in an H-bond network in the immediate vicinity of the metal center.

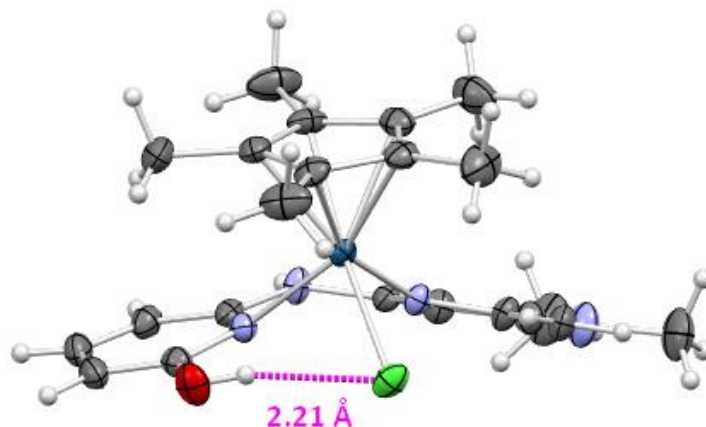


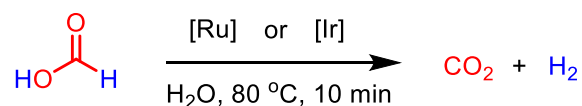
Figure 5 X-Ray molecular structure of **Ir11**. Ellipsoids are shown at 50% probability.

Formic acid dehydrogenation

Ideally, formic acid should be dehydrogenated under mild condition without the need for any additives in particular basic additives very often used for this transformation. Additives not only affect the cost and environmental impact of the process, but they can also lead to contamination of the gas stream, which will then need to be purified. In addition, it is very preferable to use highly concentrated formic acid solutions or, eventually, pure formic acid since dilution results in a decrease in volumetric energy content (1 L of pure FA stores 26.5 mole of H₂ whereas 1 L of a 3

M solution of FA stores only 3 mole of H₂). To date only very few catalysts have been reported to meet these very challenging experimental conditions.^{17,19}

All the complexes synthesized have been evaluated in the catalytic dehydrogenation of formic acid in the absence of any additives (Scheme 1).



Scheme 1 Formic acid dehydrogenation

Ruthenium complexes were first examined in water at 80 °C with a low catalyst loading of 0.01 mol% and their performances compared to the previously reported (Ru(dipyridylamine)(η^6 -p-cymene))OSO₃) **Ru1**.^{15b} As depicted in Table 2, **Ru4** and **Ru5** displayed improved performance and highlighted the benefit resulting from the introduction of a second dimethylamino-substituent on the dipyridylamine ligand. Disappointingly the use of the more electron rich Cp* ligand did not induce a major benefit as **Ru2** was only slightly more efficient than **Ru1**. Nevertheless, this matter of fact also questions the influence of the counter-ion, SO₄²⁻ for **Ru1** vs PF₆⁻ for **Ru2**. Finally, another insight of these results concerns the crucial role of the bridging amine of the dipyridylamine ligand, as the tertiaryamine-bridged **Ru3** was found to be poorly active for the dehydrogenation of FA. This information is crucial as it will be developed later.

Table 2 Dehydrogenation of formic acid with ruthenium complexes^a

Entry	Catalyst	TOF (h ⁻¹) ^b
1	Ru1	338
2	Ru2	388
3	Ru3	92
4	Ru4	614
5	Ru5	799

Conditions: ^aFA (4 mmol, 2 M), catalyst (0.01 mol%), H₂O (2 mL), 80 °C. ^bbased on gas volume released and measured with a digital flowmeter at t = 10 min. All reactions were duplicated without significant variations (\pm 5%)

Iridium catalysts were more thoroughly investigated as they are known to achieve higher performances than ruthenium catalysts. The same trend observed with ruthenium catalysts has emerged here. The electron donating group -NMe₂ on the dpa ligand brought higher TOFs (**Ir8**>**Ir7**>**Ir3**, Table 3 entries 2, 6, 7). The highest activity ever obtained with an Ir-dipyridylamine catalyst was thus achieved with **Ir8** (20441 h⁻¹). This catalyst led to full conversion of FA in 35 min (TON 10000). The iridium chloride **Ir2** was not very active for this reaction although the two dimethylamino-groups improved somehow the activity (Table 3, entry 1) when compared to **Ir1** bearing an unsubstituted dpa ligand (**Ir1**, TOF = 3047 h⁻¹). Steric hindrance at the iridium center also influences the performance of the catalysts. Catalyst **Ir4** with methyl substituents at the 6,6'-positions was the least active of all the catalysts prepared and displayed poorer performances than the unsubstituted catalyst **Ir3**. Interestingly, the -OMe group at the 6,6' positions of the catalyst **Ir5** achieved an excellent TOF of 13064 h⁻¹. This result can be the result of the lower steric hindrance and greater electron-donating effect of -OMe vs -Me. The potential involvement of the -OMe groups as acceptors of proton for H-bonds may also be considered.²⁴ The deleterious effect

of a tertiary amine-bridged dpa ligand was here again evidenced with the poor activity displayed by **Ir6** (Table 3, entry 5) as well as the poor reactivity of iridium chloride catalyst observed upon comparing the activity of **Ir2** and **Ir8** (Table 3, entries 1 and 7).

Table 3 Dehydrogenation of formic acid with iridium complexes^a

Entry	Cat	TOF (h ⁻¹) ^b	Time to full conversion (TON = 10000)
1	Ir2	7439	n.d.
2	Ir3	8705	140 min
3	Ir4	2121	n.d.
4	Ir5	13064	n.d.
5	Ir6	3382	n.d.
6	Ir7	11680	90 min
7	Ir8	20441	35 min

Conditions: ^aFA (4 mmol), catalyst (0.01 mol%), H₂O (2 mL), 80 °C. ^bbased on gas volume released and measured with a digital flowmeter at t = 10 min. All reactions were duplicated without significant variations (\pm 5%). n.d. = not determined

The performances of the hydroxy-functionalized complexes **Ir12-Ir14** were evaluated under identical conditions. As depicted in Table 4, all three catalysts displayed high activity but they did not reach the performances of **Ir8**. Comparison of **Ir13** (TOF 6301 h⁻¹) with **Ir3** (TOF 8705 h⁻¹) did not evidence an influence of the hydroxyl substituent. Albeit the di-hydroxy-substituted **Ir12** displayed a higher activity (TOF 9900 h⁻¹) than **Ir3** (TOF 8705 h⁻¹) bearing a non-substituted dpa ligand, comparison with the di-methoxy-substituted **Ir5** (TOF 13064 h⁻¹) clearly demonstrate that this improvement is unlikely due to H-bond contribution.

Only in the case of **Ir14** the introduction of a hydroxyl substituent brought an improvement when compared the hydroxyl-free **Ir7**, with a TOF of 13064 h⁻¹ vs 11680 h⁻¹. Catalyst **Ir14** led to full conversion of FA (TON = 10000) after 70 minutes. The benefit of this mixed electron-donating/Hydroxy-substitution was already evidenced with an iridium-bipyridine catalyst in the reduction of HMF.²⁵

Table 4 Dehydrogenation of formic acid with hydroxyl-containing iridium complexes ^a		
Entry	Cat (mol%)	TOF (h ⁻¹) ^b
1	Ir12	9990
2	Ir13	6301
3	Ir14	13064

Conditions: ^aFA (4 mmol), catalyst (0.01 mol%), H₂O (2 mL), 80 °C. ^bbased on gas volume released and measured with a digital flowmeter at t = 10 min. All reactions were duplicated without significant variations (\pm 5%).

Following the thorough study of the structure/activity relationship of the numerous ruthenium and iridium complexes, some important conclusions could be drawn. In particular, the poor performances of Ir-chloride catalysts and of those bearing a *N*-benzyl-bridged dipyridylamine ligand was evidenced, corroborating previous observations.¹⁵ Disappointingly, the hydroxyl-substituted dipyridylamine ligand brought only slight improvement that cannot be unambiguously attributed to the hydrogen-bond donor. This study identified the catalyst equipped with the most electron-donating dipyridylamine ligand **Ir8** as the most active catalyst.

Further studies were therefore undertaken with this catalyst, beginning with the study of its stability under repeated additions of formic acid. This study was performed using the conditions depicted here above (FA (4 mmol), catalyst (0.01 mol%), H₂O (2 mL), 80 °C) and assessing the increase in reaction time required at each run to achieve full conversion of formic acid. As depicted in Figure 6, the second run led to identical performances than the first one (TOF~20500 h⁻¹, full

conversion of FA in 38 minutes) but subsequent cycles evidenced a slow decomposition of the catalyst leading to a TOF of 16557 min^{-1} (at 10 min.) and a full conversion of FA after 48 minutes for the 6th cycle. It is worth noting that, despite a slow erosion of performance, the results achieved in the 6th run still outperform those of the other iridium catalysts described earlier.

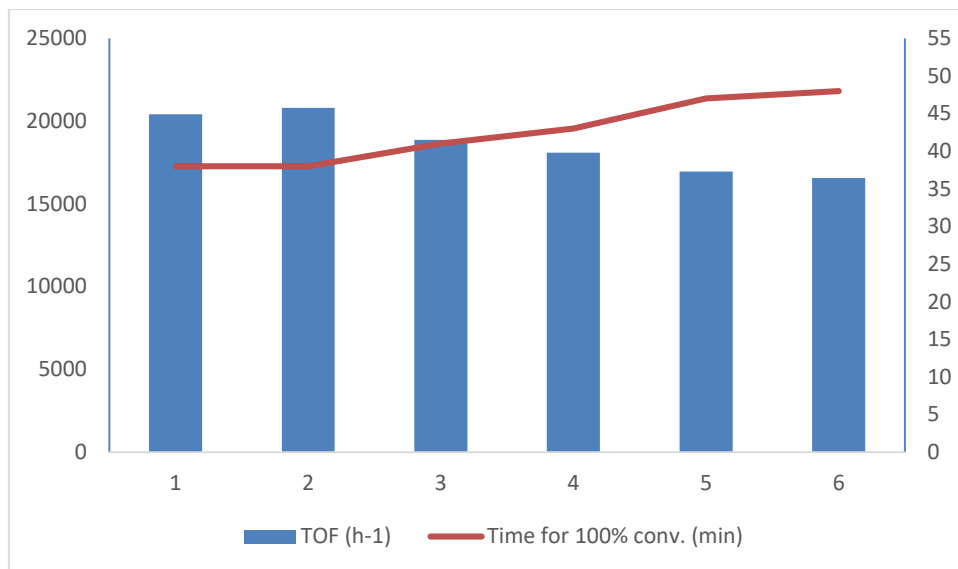


Figure 6 : Consecutive reuse of Ir8 (Initial load of **Ir8**. FA reloaded after full conversion in the previous run)

We next investigated the performance under various concentration conditions (Figure 7). With concentrations ranging from 2 M to 8 M, TOFs higher than 17213 h^{-1} (in 8 M) were reached, with a maximum TOF of 21205 h^{-1} obtained for a concentration of 3 M. At this concentration a TON of 474000 corresponding to the release of 9.2 L of gas was reached upon repeated addition of FA over 52 h. A lower concentration (1 M) caused the activity to drop to 13156 h^{-1} . Most importantly, the reaction in neat formic acid (26,5 M) proceeded with a TOF of 11373 h^{-1} . Although this result is less favorable than those found in water, it nevertheless shows that a base-free dehydrogenation of neat formic acid, a method with great potential for producing hydrogen, is feasible. Those results

are almost two times higher than those previously obtained with **Ir7**¹⁷ evidencing again the influence of the electron donating property of the ligand. These results make **Ir8** one of the most active catalysts for the dehydrogenation of pure formic acid under base-free conditions. Milstein recently reported a maximum TOF of 3067 h⁻¹ at 95 °C for the base-free dehydrogenation of neat formic acid with a ruthenium catalyst^{19a} while Gelman reported a TOF of 11760 h⁻¹ at 70 °C for the same reaction using an iridium pincer-complex.^{19b} It should also be mentioned that the dimethylamino-substituted bipyridine iridium catalyst recently reported by Himeda was not active for the dehydrogenation of neat formic acid.²⁶

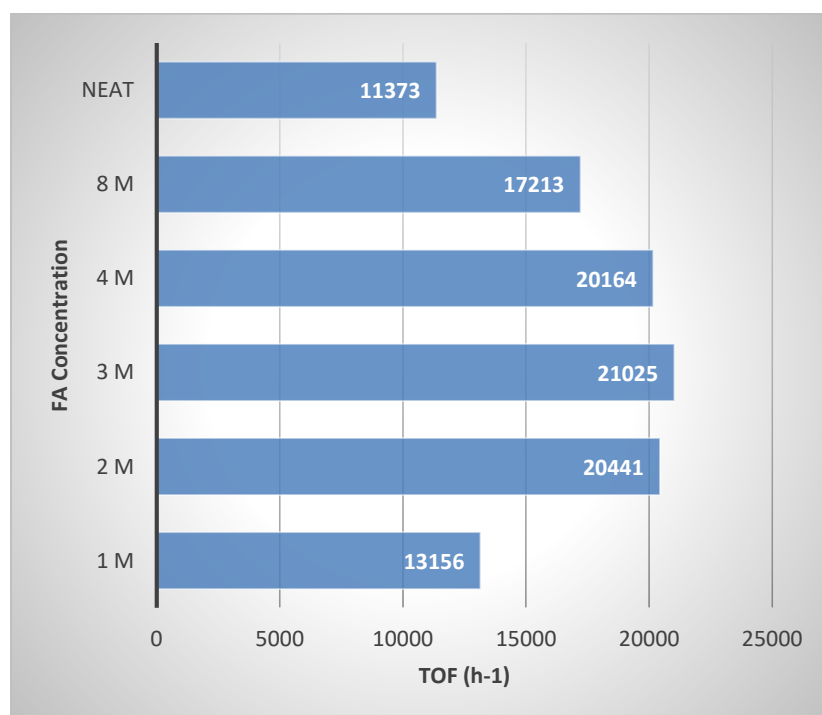


Figure 7 Influence of the concentration on the activity of the base-free dehydrogenation of FA.

The influence of the pH on the reaction outcome was further investigated. Before going into the details of this study, it is important to discuss the stability of **Ir8** under acidic conditions since **Ir8**

incorporates amino-groups in the dpa ligand. As discussed above, the X-ray structure of **Ir8** revealed planar or nearly planar amino-groups indicating the delocalization of the nitrogen lone pair on the pi-system, hence suggesting a very weak basic character of these amino groups. To further confirm this prediction, **Ir8** was mixed with various amounts of acetic acid (1-10 equiv., pKa 4.78) in dms-*d*₆ at different temperatures (r.t. to 80 °C) for different times (5 minutes to 1 h). The evolution of these solutions was followed by ¹H NMR and, as anticipated, none of the conditions tested showed any decomposition or evolution of **Ir8** (See ESI). A pH-dependence study on the initial TOFs was then conducted using mixtures of formic acid and sodium formate in varying proportions (Table 5). The results showed that the highest TOF of 28678 h⁻¹ was achieved at pH = 3.2 (Table 5, entry 2). In contrast, catalytic activity was almost inhibited at neutral pH of 7.4 where a low TOF value of 1291 h⁻¹ was obtained. These results are similar to those obtained with other iridium complexes bearing bipyridine or bis-*N*-heterocyclic ligands for which the best TOFs were obtained at pH 3.5-4 (i.e. ~ pKa of formic acid). They also confirm that acidic media is required and that formate improves the catalyst activity to a limited extent. In fact, TOFs at pH 1.8 (no base) and 3.8 (pH≈pKa) are quite similar (Table 5, entries 1&3). Given the cost of bases²⁷ and the associated waste management, as well as the problem of potential contamination of the generated gas stream, we believe that base-free conditions are highly preferable.

Table 5 Dehydrogenation of formic acid with iridium complexes at different pH ^a				
Entry	Cat (mol%)	FA/HCOONa	pH ^b	TOF (h ⁻¹) ^c
1	Ir8	4: 0	1.8	20441
2	Ir8	3: 1	3.2	28678
3	Ir8	2: 2	3.8	21824
4	Ir8	1: 3	4.4	12141
6	Ir8	0: 4	7.4	1291

Conditions: ^aFA (4 mmol), catalyst (0.01 mol%), H₂O: 2 ml, 80 °C. ^bpH values were measured with a pH meter. ^cbased on gas volume released and measured with a digital flowmeter at t = 10 min. All reactions were duplicated without significant variations (± 5%)

The temperature dependency of the catalytic activity was examined over a temperature range from 60 to 100 °C in aqueous solutions of FA (3 M), (Table 6). Of note, it was shown that the catalyst was still active at a temperature as low as 60 °C and at 90 °C with a catalyst loading of 10 ppm resulting in a TOF of 39274 h⁻¹. However, in the latter case, full conversion of formic acid could not be reached as the gas flow stopped after 3 h corresponding to a TON of 84453 (Table 6, entry 5, TON th. = 100000). The highest TOF values were found at 100 °C, and remarkably, a TOF of 66639 h⁻¹ was recorded for the base-free dehydrogenation of FA at this temperature using a very low catalyst loading of 0.005 mol% (50 ppm, Table 6, entry 6). This is a 75% improvement with regard to **Ir7** for which a TOF of 38236 h⁻¹ was obtained under identical conditions. From those results, we could calculate an experimental activation energy of 18.5 kcal.mol⁻¹ (see details in ESI).

Table 6 Dehydrogenation of formic acid with Ir8 at different temperature ^a			
Entry	Cat (mol%)	Temp.	TOF (h ⁻¹) ^b
1	Ir8 (0.01)	60	4119
2	Ir8 (0.01)	70	12295
3	Ir8 (0.01)	80	21516
4	Ir8 (0.01)	90	35700
5	Ir8 (0.001)	90	39274
6	Ir8 (0.005)	100	66639

Conditions: ^a FA (4 mmol), catalyst (mol%), H₂O (1.3 mL), 5 min. ^bbased on gas volume released and measured with a digital mass flowmeter. All reactions were duplicated without significant variations (\pm 5%)

Fuel cells generate electricity using hydrogen as fuel releasing water as the sole effluent. For proper operation and longevity of the fuel cell, the purity of the gas feed must be good enough and free of contaminants, in particular CO which can be generated by FA dehydration. Indeed, the

CO content of gas stream must be very low as even minute quantities of carbon monoxide can poison the platinum electrodes that are key to driving the fuel cell.²⁸ Hence the gas flow generated by formic acid dehydrogenation must be free of CO or containing less than 10 ppm of CO. In order to improve previous experimental setup and procedure in which measurements were acquired only at the very beginning of a dehydrogenation process, the flowmeter was connected to a gas chromatography apparatus equipped with a catharometer detector. With this setup, CO levels could be monitored all along the dehydrogenation, i.e., up to high and full conversions. It is indeed a rather usual feature in catalysis to have very selective transformation at low conversion with further selectivity erosion at higher conversions. With this device, the CO content of the gas stream from the dehydrogenation at 80 °C of a 3 M formic acid solution was monitored at 1 min, 15 min and 30 min. Satisfactorily, CO was not detected in any of these measurements, ensuring that the CO level in the gas stream was below the detection limit of the analysis, i.e. below 1 ppm. Similarly, no CO could be detected for the dehydrogenation of neat formic acid (see ESI).

Although generation of high pressure of H₂²⁹ may have an interest in some domains, fuel cells generally require moderate hydrogen pressure.³⁰ The possibility to generate moderate pressure of hydrogen by dehydrogenation of FA with **Ir8** was investigated by performing the dehydrogenation in a high pressure reactor. For this purpose, a 3 M solution of formic acid and **Ir8** was heated at 80 °C in a Parr reactor. A pressure of 60 bar, sufficient to feed a fuel-cell, was generated within 1 h and did not further evolve suggesting that equilibrium was reached.

Formic acid being foreseen as a hydrogen reservoir, the question of hydrogen release in remote locations must be considered. In particular, for mobile application, the end-user should be able to generate hydrogen in the simplest possible way without proceeding to any complex manipulation or FA/catalyst mixing. Premixing FA and catalyst would constitute an attractive option requiring

a long-term catalyst stability in the presence of FA. Catalysts exhibiting this property are often referred as latent or dormant catalysts. They are of particular interest in polymer chemistry.³¹ Several studies on this type of catalyst have also been reported in olefin metathesis.³² To evaluate the latent character of **Ir8**, a stock solution of this complex (0.01 mol%) in 1.5 mL of FA was prepared and stored at ± 4 °C. An aliquot was removed after two days and diluted with water to a FA concentration of 3 M. This solution was submitted to the dehydrogenation procedure at 80 °C resulting in a TOF of 20594 h⁻¹. This procedure was repeated after 10 days leading to a TOF of 20133 h⁻¹. It is remarkable that in both cases, only a small TOF drop was observed when compared to the TOF of 21025 h⁻¹ recorded under standard conditions. This outcome shows that the catalyst **Ir8** is very stable in pure formic acid at moderately low temperature and therefore suitable for premixing with FA before being transported and used.

Having demonstrated the high stability of the catalyst in FA, we have also evaluated its recyclability using the generated pressure as a probe (3 M in H₂O, Figure 8). After a first run delivering 60 bar of pressure, the reactor was gently depressurized and reloaded with fresh FA. Upon heating at 80 °C the pressure reached 60 bar within 1.5 h. The next recycling showed a decrease of the activity as lower pressure of 55 bar and 50 bar were reached within 2 h and 3 h, respectively. Albeit not sufficient to envision of multiple reuse of the catalyst, these results confirm the very high stability of the catalyst under acidic conditions.

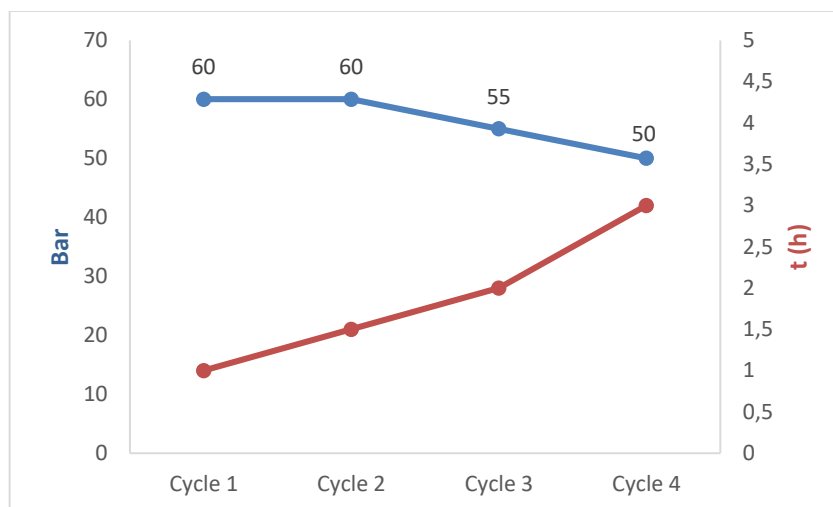
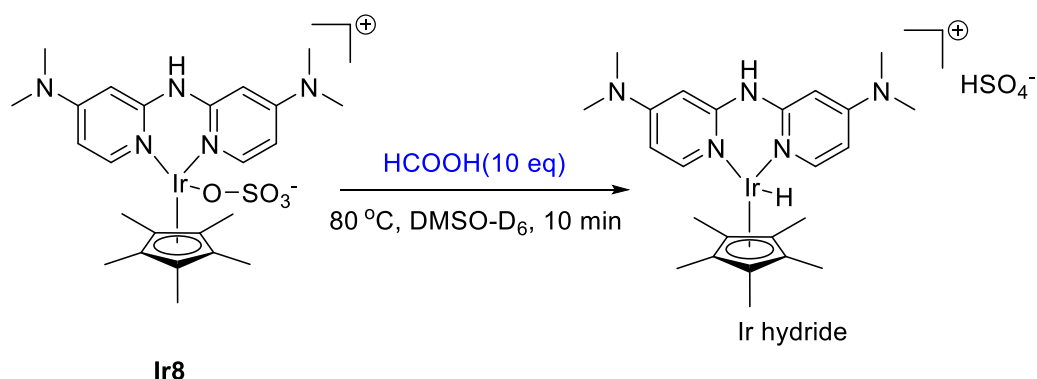


Figure 8 Catalyst reuse

Reaction mechanism

Several studies on the mechanism of HCOOH dehydrogenation by transition-metal catalysts have been reported.²² While many mechanisms share common features, they may differ, for example, in the use of base additives. In all cases, metal-hydrides complexes are key species in the mechanism. These metal-hydrides are obtained by β -hydride elimination or direct hydride-transfer involving a formate species formed in the presence of a base such as triethylamine or using formic acid/sodium formate mixtures. In the absence of base, the formation of the metal hydride species involves the deprotonation of formic acid by the catalyst ligand or alternatively by a preformed metal-hydride species.^{19,22} With these considerations in mind, we initiated the investigation of the reaction mechanism both experimentally and theoretically using DFT calculations. First, we looked at the synthesis and characterization of a potential Ir-hydride intermediate. For this purpose, a mixture of **Ir8** and 10 equiv. of FA in DMSO-*d*₆ was heated at 80 °C for 10 minutes and then analyzed by ¹H NMR. This NMR revealed the clean formation of a metal hydride complex observed as a singlet at -10.33 ppm (see ESI). The NMR data are in agreement with the structure

depicted in scheme 2. Unfortunately, we could not isolate this hydride species for further characterization. Incidentally, this result is further evidence of the stability of **Ir8** under acidic conditions.



Scheme 2 Formation of Iridium hydride species

Kinetic Isotope Effect experiments were carried out using deuterated formic acid and/or deuterated water in order to identify the rate determining step of the reaction. As depicted in Table 7, the rate of dehydrogenation of formic acid was only slightly impacted in D₂O. To the contrary, the rate of dehydrogenation of deuterated formic acid in H₂O showed a significant KIE of 3.3 which was further increased in D₂O. These results indicate that cleaving a bond to deuterium is involved in the rate-determining step of the reaction. This could either be the cleavage of the C-D bond in formic acid to generate the Ir-D species or the cleavage of this Ir-D species to release HD or D₂.

KIE experiments in neat formic acid were also performed and demonstrated that under this solvent-free condition, nor the CH or OH group of FA are involved in or before the rate determining step (Table 7, entries 5,6).

Table 7 Kinetic isotope effect (KIE) in the dehydrogenation of formic acid with **Ir8**^a

Entry	Source	Solvent	TOF (h ⁻¹) ^b	KIE
1	HCOOH	H ₂ O	20686	- (reference)
2	HCOOH	D ₂ O	12326	1.7
3	DCOOD	H ₂ O	6270	3.3
4	DCOOD	D ₂ O	5010	4.1
5	HCOOH	--	11127	
6	DCOOD	--	7469	1.5

Conditions: ^a FA (4 mmol), catalyst (mol%), H₂O (1.3 mL), 5 min. ^b based on gas volume released.

DFT calculations were undertaken to investigate the reaction energy profile. Several key results were considered to establish a working hypothesis. First, having established that the dpa ligand is not intrinsically basic, we have hypothesized that SO₄²⁻, albeit very poorly basic could play the role of a base to deprotonate coordinated formic acid. We made this assumption previously,^{15b} and interestingly, Li and coworkers confirmed this hypothesis by DFT when studying several iridium catalyst including ours in the hydrogenation of levulinic acid into γ -valerolactone.³³ Secondly, the importance of the bridging N-H moiety in the dpa ligand was considered to establish H-bonding interactions. An energetic profile of the reaction is presented in Figure 9(a) (for full details of DFT calculation, see ESI). Starting from the zwitterionic complex **Ir8** in water, the first step consists in the substitution of OSO₃ anion by a molecule of water. Of note the SO₄ anion may remain bonded to the iridium complexes by H-bonding with water or with the bridging N-H of the ligand (**Int2** and **Int2'**). Deprotonation of formic acid by SO₄²⁻ then leads to the formation of the formate intermediates **Int3** and **Int3'** of similar energy. The formation of an iridium-hydride complex through a TS involving a β -hydride elimination could not be located in contrast to a direct hydride

abstraction in **TS1** leading to **Int5** and **Int5'** with release of CO₂. Note that a pathway involving a concerted formic acid deprotonation with direct-hydride abstraction was not found favorable (see ESI). It is also noteworthy that **Int5''** not involving HSO₄⁻ was found 5.6 kcal.mol⁻¹ higher than **Int5'** (Figure 9, (a)-1). The two intermediates **Int5** and **Int5'** then release H₂ through **TS2** or **TS2'** involving water or formic acid as hydrogen shuttles, respectively. Calculations showed that the formic acid-assisted hydrogen release pathway (8.8 kcal.mol⁻¹ for **TS2'**) is preferred to the water-assisted hydrogen release (15.0 kcal.mol⁻¹ for **TS2**). Overall, this theoretical study allows to draw remarkable characteristics of the mechanism which corroborate experimental observations. In particular, the role of the bridging N-H in establishing H-bonding is evidenced along with the role of the SO₄ anion. This theoretical study identifies the hydride formation as the rate determining step with an activation energy of 18.5 kcal.mol⁻¹ which fits perfectly well with the experimental value of 18.5 kcal.mol⁻¹ (vide supra). An Eyring analysis of the experimental results reported here above revealed activation parameters of $\Delta H^\ddagger = 18.2 \text{ kcal.mol}^{-1}$ and $\Delta S^\ddagger = -33 \text{ cal.mol}^{-1}.\text{K}^{-1}$ (see ESI). This negative entropy of activation is consistent with an associative pathway leading to **TS1** either from **Int3** as well as **Int3'** since numerous attempts to calculate **TS1** always located the HSO₄⁻ anion in the close vicinity of the dpa ligand. Having identified the rate determining step with **Ir8**, we have looked as this same TS with **Ir3** which is not equipped with a strong electron-donating dipyridylamine ligand. In line with the experimental results, a higher activation energy of 21.4 kcal.mol⁻¹ was calculated (see ESI). The overall catalytic cycle is depicted in Figure9(b).

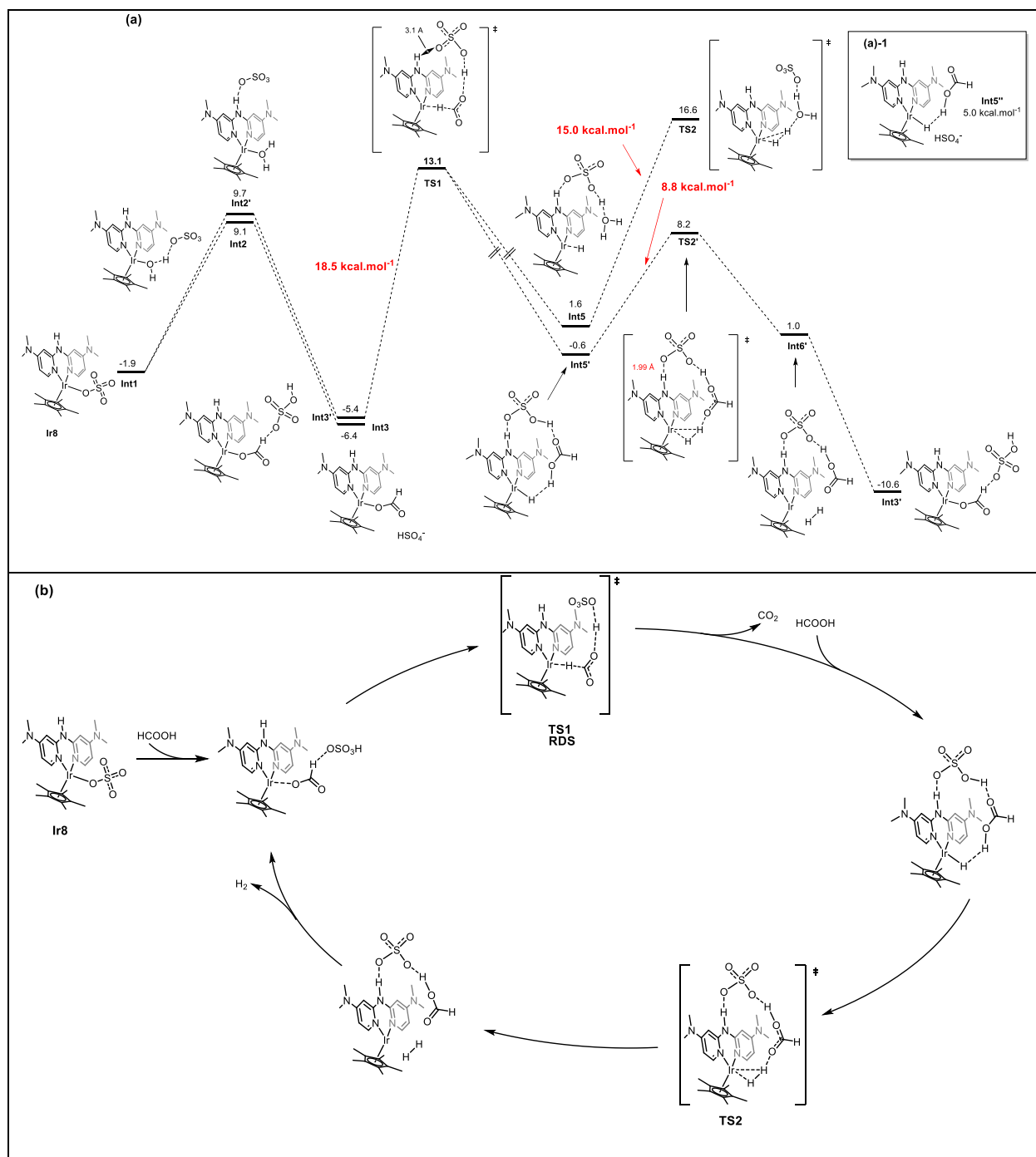


Figure 9 (a) DFT calculated energy profile for the dehydrogenation of formic acid in water by Ir8 at 353 K . Relative free energy (kcal.mol⁻¹), (M06L, def2TZVP, SMD solvent model with water)

CONCLUSION

We have synthesized numerous new ruthenium and iridium complexes incorporating electron-donating ligands in their coordination sphere. From all these complexes, the iridium complex **Ir8** bearing a bis-dimethylamino-substituted dipyridylamine ligand was found the most efficient for the dehydrogenation of formic acid without requirement of base additives. Contrary to many catalysts reported so far, **Ir8** is an air-stable complex than can be used in water without strict exclusion of air. The study was conducted at 80 °C in water media (3 M FA, TOF = 21516 h⁻¹), but the catalyst was also active at lower temperature down to 60 °C. The highest TOF of 66639 h⁻¹ was achieved at 100 °C with a catalyst loading of 50 ppm (0.005 mol%). Notably, **Ir8** could also perform the dehydrogenation of neat formic acid achieving one of the highest TOF obtained without any additives (11373 h⁻¹). Beside the catalytic performances, the catalyst was shown to be selective as carbon monoxide could not be detected in the gas stream from the beginning to the end of the dehydrogenation of a 3 M solution of formic acid. In addition, when implemented in a closed system, a pressure of 60 bar could be easily reached. Experimental and theoretical mechanistic investigations highlighted the key role of the SO₄ anion as well as the bridging -NH- of the dipyridylamine ligand in a mechanism where H-bonding and proton-shutteling are involved. Of note, DFT calculations show that the rate determining step of the reaction is the formation of an iridium hydride species. Hence, if the strategy of electron enrichment of the metal center turned to be successful, it is not due to the increase of hydricity of the metal-hydride species. Last but not least we have demonstrated the very high stability of the catalyst in acidic media. Thanks to this, it is possible to store a premix of formic acid and catalyst at moderately low temperature (+ 4-5 °C) for a couple of day before proceeding to dehydrogenation which occurs with almost no

decrease of performance. We believe that this characteristic could be very useful for the development of hydrogen mobility.

Supporting Information.

Experimental details for ligand and complexes syntheses and characterization. Experimental details formic acid dehydrogenation; Theoretical calculation details.

AUTHOR INFORMATION

Corresponding Author

Cédric Fischmeister, Univ Rennes, CNRS, ISCR (Institut des Sciences Chimiques de Rennes) – UMR 6226, 35042 Rennes, France. E-mail : cedric.fischmeister@cnrs.fr. <https://orcid.org/0000-0002-9490-8145>

Author Contributions

The manuscript was written through contributions of all authors. All authors have given approval to the final version of the manuscript.

Notes

Any additional relevant notes should be placed here.

ACKNOWLEDGMENT

The authors are grateful to the China Scholarship Council for a grant to LG. The authors also thank M. Thierry Labasque from the platform “Condate Eau” (OSUR-Université de Rennes 1) for the loan of GC equipment for gas analyses.

REFERENCES

¹ (a) Skilhagen, S. E.; Dugstad, J. E.; Aaberg, R. J. Osmotic power - power production based on the osmotic pressure difference between waters with varying salt gradients. *Desalination*, **2008**, *220*, 476-482; (b) Helfer, F.; Lemckert, C.; Anissimov, Y. G. Osmotic power with Pressure Retarded Osmosis: Theory, performance and trends - A review. *J. Membr. Sci.*, **2014**, *453*, 337-358.

² (a) Bockris, J. O. A hydrogen economy. *Science* **1972**, *176*, 1323; (b) Bockris, J. O. The hydrogen economy: Its history. *Int. J. Hydrogen Energ.* **2013**, *38*, 2579-2588; (c) Brandon N. P.; Kurban, Clean energy and the hydrogen economy. *Z. Phil. Trans. R. Soc. A*, 2017, 375, 20160400.

³ Turner, J. A. *Science* **1999**, *285*, 687–689.

⁴ (a) Deuss, P. J.; Barta, K.; de Vries, J. G. Homogeneous catalysis for the conversion of biomass and biomass-derived platform chemicals. *Catal. Sci. Technol.* **2014**, *4*, 1174-1196; (b) Barta, K.; Ford, P. C. Catalytic Conversion of Nonfood Woody Biomass Solids to Organic Liquids. *Acc. Chem. Res.* **2014**, *47*, 1503-1512.

⁵ Chatenet, M.; Pollet, B. G.; Dekel, D. R.; Dionigi, F.; Deseure, J.; Millet, P.; Braatz, R. D.; Bazant, M. Z.; Eikerling, M.; Staffell, I.; Balcombe, P.; Saho-Horn, Y.; Schäfer, H. *Chem. Soc. Rev.* **2022**, *51*, 4583-4762.

⁶ (a) Panchenko, V., A.; Daus, Y. V.; Kovalev, A. A.; Yudaev, I. V.; Litti, Y. V. Prospects for the production of green hydrogen: Review of countries with high potential. *Int. J. Hydrogen. Energ.* **2023**, *48*, 4551-4571; (b) Zhu, B.; Wei, C. A green hydrogen era: Hope or hype. *Environ. Sci. Technol.* **2022**, *56*, 11107-11110; (c) Yu, M.; Wang, K.; Vredenburg, H. Insights into low-carbon hydrogen production methods: Green, blue and aqua hydrogen. *Int. J. Hydrogen. Energ.* **2021**, *46*, 21261-21273.

⁷ (a) Andersson J.; Grönkvist S. Large-scale storage of hydrogen. *Int. J. Hydrogen Energ.*, **2019**, *44*, 11901-11919; (b) Abe J.O.; Popoola A.P. I.; Ajenifuja E.; Popoola O. M. Hydrogen energy, economy and storage: Review and recommendation. *Int. J. Hydrogen Energ.*, **2019**, *44*, 15072-15086.

⁸ (a) Niermann M.; Beckendorff A.; Kaltschmitt M.; Bonhoff K. Liquid Organic hydrogen Carrier (LOHC) - Assessment based on chemical and economic properties. *Int. J. Hydrogen Energy*, **2019**, *4*, 6631-6654; (b) van Putten R., Wissink T., Swinkels T.; Pidko E. A. Fuelling the hydrogen economy: Scale-up of an integrated formic acid-to-power system, *Int. J. Hydrogen Energ.* **2019**, *44*, 28533-28541; (c) Preuster P., Papp C.; Wasserscheid P. Liquid Organic Hydrogen Carriers (LOHCs): Toward a hydrogen-free hydrogen Economy *Acc. Chem. Res.*, **2017**, *50*, 74-85.

⁹ (a) Onishi, N.; Kanega, R.; Kawanami, R.; Himeda, Y. Recent progress in homogeneous catalytic dehydrogenation of formic acid. *Molecules*, **2022**, *27*, 455; (b) Guo J.; Yin C. K.; Zhong D. L.; Wang Y. L.; Qi T.; Liu G. H.; Shen L. T.; Zhou Q. S.; Peng Z. H.; Yao H.; Li X. B. Formic acid as a potential on-board hydrogen storage method: Development of homogeneous Noble Metal Catalysts for dehydrogenation Reactions *ChemSusChem*, **2021**, *14*, 2655-2681; (c) Iglesias M.;

Fernandez-Alvarez F. J. Advances in non-precious metal homogeneously catalyzed formic acid dehydrogenation *Catalysts*, 2021, **11**, 1288; (d) Guan C.; Pan Y.; Zhang T.; Ajitha M. J.; Huang K.-W. An Update on formic acid dehydrogenation by homogeneous catalysis. *Chem. Asian J.*, **2020**, *15*, 937-946 Sordakis K.; Tang C.; Vogt L. K.; Junge H.; Dyson P. J.; Beller M.; Laurenczy, G. homogeneous catalysis for sustainable hydrogen storage in formic acid and alcohols. *Chem. Rev.* **2018**, *118*, 372-433; (e) Graseman M.; Laurenczy G. formic acid as a hydrogen source – recent developments and future trends. *Energy Environ. Sci.* **2012**, *5*, 8171-8181; (f) Wang W.-H.; Himeda Y.; Muckerman J. T.; Manbeck G. F.; Fujita E. CO₂ Hydrogenation to formate and methanol as an Alternative to photo- and electrochemical CO₂ reduction. *Chem. Rev.* **2015**, *115*, 12936-12973.

¹⁰ (a) Bulushev, D. A.; Ross, J. R. H.; Towards sustainable production of formic acid. *ChemSusChem* **2017**, *11*, 821-836; (b) Chen, X.; Liu, Y.; Wu, J. Sustainable production of formic acid from biomass and carbon dioxide. *Molec. Catal.* **2020**, *483*, 110716.

¹¹ For examples of formic acid dehydrogenation with base additives, see: (a) Lentz N.; Albrecht M. A Low-coordinate iridium complex with a donor-flexible O,N-ligand for highly efficient formic acid dehydrogenation, *ACS Catal.*, **2022**, *12*, 12627-12631; (b) Celaje J. J. A.; Lu Z.; Kedzie A. E.; Terrile N. J.; Lo J. N.; Williams T. J.; A prolific catalyst for dehydrogenation of neat formic acid, *Nature. Commun.* **2016**, *7*, 11308; Wang W.-H.; Ertem M. Z.; Xu S.; Onishi N.; Manaka Y.; Suna Y.; Kambayashi H.; Muckerman J. T.; Fujita E.; Himeda Y. Highly robust hydrogen generation by bioinspired Ir complexes for dehydrogenation of formic acid in water: experimental and theoretical mechanistic investigations at different pH. *ACS Catal.*, **2015**, *5*, 5496-5504.

¹² Wang, D.; Astruc D. The golden age of transfer hydrogenation. *Chem. Rev.* **2015**, *115*, 6621-6686.

¹³ Wang, S.; Bruneau, C.; Renaud, J.-L., Gaillard, S., Fischmeister, C. 2,2'-Dipyridylamines: more than just sister members of the bipyridine family. Applications and achievements in homogeneous catalysis and photoluminescent materials. *Dalton Trans.*, **2019**, *48*, 11599-11622.

¹⁴ (a) Pileidis, F. D.; Titirici, M.-M. Levulinic acid biorefineries: New challenges for efficient utilization of biomass. *ChemSusChem*, **2016**, *9*, 562-582; (b) Omoyuri, U.; Page, S.; Hallett, ; Miller, P. W.; Homogeneous catalyzed reactions of levulinic acid: To γ -valerolactone and beyond. *ChemSusChem*, **2016**, *9*, 2037-2047.

¹⁵ a) Wang, S.; Dorcet, V.; Roisnel, T.; Bruneau, C.; Fischmeister, C.; Ruthenium and iridium dipyridylamine catalysts for the efficient synthesis of γ -valerolactone by transfer hydrogenation of levulinic acid. *Organometallics*, **2017**, *36*, 708-713 ; b) Wang, S.; Huang, H.; Dorcet, V.; Roisnel, T.; Bruneau, C.; Fischmeister, C. Efficient iridium catalysts for base-free hydrogenation of levulinic acid. *Organometallics*, **2017**, *36*, 3152-3162.

¹⁶ a) Wang, S.; Huang, Bruneau, C.; Fischmeister, C. Selective and efficient iridium catalyst for the reductive amination of levulinic acid into pyrrolidones. *ChemSusChem* **2017**, *10*, 4150-4154; b) Wang, S.; Huang, Bruneau, C.; Fischmeister, C. Formic acid as a hydrogen source for the iridiumcatalyzed reductive amination of levulinic acid and 2-formylbenzoic acid. *Catal. Sci. Technol.* **2019**, *9*, 4077-4082.

¹⁷ S. Wang, H. Huang, T. Roisnel, C. Bruneau, C. Fischmeister. Base-Free Dehydrogenation of Aqueous and Neat Formic Acid with Iridium(III) Cp*(dipyridylamine) Catalysts. *ChemSusChem*, **2019**, *12*, 179-184.

¹⁸ For examples of dehydrogenation of formic acid without basic additives, see: (a) Himeda Y. Highly efficient hydrogen evolution by decomposition of formic acid using an iridium catalyst with 4,4'-dihydroxy-2,2'-bipyridine. *Green Chem.* **2009**, *11*, 2018-2022; (b) Boddien A.; Mellmann D.; Gartner F.; Jackstell R.; Junge H.; Dyson P. J.; Laurenczy G.; Ludwig R.; Beller M. Efficient dehydrogenation of formic acid using an iron catalyst. *Science* **2011**, *333*, 1733-1736; (c) Manaka Y.; Wang W.-H.; Suna Y.; Kambayashi H.; Muckerman J. T.; Fujita E.; Himeda Y. Efficient H₂ generation from formic acid using azole complexes in water. *Catal. Sci. Technol.* **2014**, *4*, 34-37; (d) Vogt M.; Nerush A.; Diskin-Posner Y.; Ben-David Y.; D. Milstein, Reversible CO₂ binding triggered by metal–ligand cooperation in a rhenium(I) PNP pincer-type complex and the reaction with dihydrogen. *Chem. Sci.* **2014**, *5*, 2043-2051; (e) Bertini F.; Mellone I.; Ienco A.; Peruzzini M.; Gonsalvi L. Iron(II) Complexes of the linear rac-tetraphos-1 ligand as efficient homogeneous catalysts for sodium bicarbonate hydrogenation and formic acid dehydrogenation. *ACS Catal.* **2015**, *5*, 1254-1265; (f) Lu S.-M.; Wang Z.; Wang J.; Li J.; Li C. Hydrogen generation from formic acid decomposition on a highly efficient iridium catalyst bearing a diaminoglyoxime ligand. *Green Chem.* **2018**, *20*, 1835-1840; (g) Prichatz C.; Trincado M.; Tan L.; Casas F.; Kammer A.; Junge H.; Beller M.; Grützmacher H. Highly efficient base-free dehydrogenation of formic acid at low temperature. *ChemSusChem* **2018**, *11*, 3092-3095; (h) Pan Y.; Pan C.-L.; Zhang Y.; Li H.; Min S.; Guo X.; Zheng B.; Chen H.; Anders A.; Lai Z.; Zheng J.; Huang K.-W. Selective hydrogen generation from formic acid with well-defined complexes of ruthenium and phosphorus–nitrogen PNP-pincer ligand. *Chem. Asian J.* **2016**, *11* 1357-1360; (i) Curley, J. B.; Bernskoetter, W. H.; Hazari, N., Additive-free formic acid dehydrogenation Using a pincer-supported iron catalyst. *ChemCatChem* **2020**, *12*, 1934-1938; (j) Pandey, B.; Krause, J. A.; Guan, H. Iron dihydride complex stabilized by an all-phosphorus-based pincer ligand and carbon monoxide.

Inorg. Chem. **2022**, *61*, 11143-11155; (k) Léval, A.; Junge, H.; Beller, M. Manganese(I) κ^2 -NN complex-catalyzed formic acid dehydrogenation. *Catal. Sci. Technol.* **2020**, *10*, 3931–3937; (l) S. Oldenhof, M. Lutz, B. de Bruin, J. I. van der Vlugt, J. N. H. Reek. Dehydrogenation of formic acid by Ir–bisMETAMORPhos complexes: experimental and computational insight into the role of a cooperative ligand. *Chem. Sci.* **2015**, *6*, 1027-1034; (m) Bielinski E. A.; Lagaditis P. O.; Zhang Y.; Mercado B. Q.; Wertele C.; Bernskoetter W. H.; Hazari N.; Schneider S. Lewis acid-assisted formic acid dehydrogenation using a pincer-supported iron catalyst. *J. Am. Chem. Soc.* **2014**, *136*, 10234-10237; (n) Wang Z.; Lu S.-M.; Li J.; Wang J.; Li C. Unprecedentedly high formic acid dehydrogenation activity on an iridium complex with an *N,N'*-diimine ligand in water. *Chem. Eur. J.* **2015**, *21*, 12592-12595; (o) Jongbloed L. S.; de Bruin B.; Reek J. N. H.; Lutz M.; van der Vlugt J. I. Reversible cyclometalation at Rh(I) as a motif for metal–ligand bifunctional bond activation and base-free formic acid dehydrogenation. *Catal. Sci. Technol.* **2016**, *6*, 1320-1327; (p) Neary M. C.; Parkin G. Nickel-catalyzed release of H₂ from formic acid and a new method for the synthesis of zerovalent Ni(PMe₃)₄. *Dalton Trans.* **2016**, *45*, 14645-14650; C. S.; Lang, Z.; Du, J.; Du, Z.; Li, Y.; Tan, H.; Li, Y. Engineering of iridium complexes for the efficient hydrogen evolution of formic acid without additives. *J. Catal.* **2022**, *413*, 119-126.

¹⁹ For examples of neat formic acid dehydrogenation under base- and additive-free conditions, see reference 17 (a) and: (a) Kar S.; Rauch M.; Leitun G.; Ben-David Y.; Milstein D. Highly efficient additive-free dehydrogenation of neat formic acid. *Nature Catal.* **2021**, *4*, 193-201; (b) Cohen, S.; Borin, V. Schapiro, I.; Musa, S.; De-Botton, S.; Belkova, N. V.; Gelman, D. Ir(III)-PC(sp³)P Bifunctional catalysts for production of H₂ by dehydrogenation of formic acid: Experimental and theoretical study. *ACS Catal.* **2017**, *7*, 8139-8146.

²⁰ a) W.-H. Wang, M. Z. Ertem, S. Xu, N. Onishi, Y. Manaka, Y. Suna, H. Kambayashi, J. T. Muckerman, E. Fujita, Y. Himeda, *ACS Catal.*, 2015, 5, 5496; b) Y. Manaka, W.-H. Wang, Y. Suna, H. Kambayashi, J. T. Muckerman, E. Fujita, Y. Himeda, *Catal. Sci. Technol.*, **2014**, 4, 34. c) Z. Wang, S.-M. Lu, J. Li, J. Wang, C. Li, *Chem. Eur. J.*, **2015**, 21, 12592-12595 ;

²¹ (a) Pitman, C. L.; Brereton, K. R.; Miller, A. J. M. Aqueous hydricity of late metal complexes as a continuum tuned by ligands and the medium. *J. Am. Chem. Soc.* **2016**, 138, 2252-2260; (b) Brereton, K. R.; Smith, N. E.; Hazari, N.; Miller, A. J. M. Thermodynamic and kinetic hydricity of transition metal hydrides. *Chem. Soc. Rev.* **2020**, 49, 7929-7948.

²² Iglesias M.; Oro L. A. Mechanistic considerations on homogeneously catalysed formic acid dehydrogenation. *Eur. J. Inorg. Chem.* **2018**, 2125-2138

²³ Average C-N bond length is sp³ amine = 1.45 Å, in sp² amine = 1.27 Å)

²⁴ Palusiak, M.; Grabowski, S. J. Methoxy group as an acceptor of proton in hydrogen bonds. *J. Mol. Struct.* **2002**, 642, 97-104.

²⁵ A similarly modified bipyridine ligand and an iridium catalyst were reported for the transformation of HMF : Xu, Z; Yan, P; Li, H.; Liu, K.; Liu, X.; Jia, S.; Zhang, Z. C. Active Cp*Iridium(III) complex with ortho-hydroxyl group functionalized bipyridine ligand containing an electron-donating group for the production of diketone from 5-HMF. *ACS Catal.* **2016**, 6, 3784.

²⁶ Kawanami, H.; Iguchi, M.; Himeda, Y. Ligand Design for Catalytic Dehydrogenation of Formic Acid to Produce High-pressure Hydrogen Gas under Base-free Conditions. *Inorg. Chem.* **2020**, 59, 4191-4199

²⁷ Solakidou, M.; Gemenetzi, A.; Koutsikou, G.; Theodorakopoulos, M.; Deligiannakis, Y.; Louloudi, M. *Cost efficiency analysis of H₂ production from formic acid by molecular catalysts. Energies* **2023**, *16*, 1723.

²⁸ (a) Baschuk J. J.; Li X. Carbon monoxide poisoning of proton exchange membrane fuel cells. *Int. J. Energy Res.* **2001**, *25*, 695-713 (b) Scott F. J.; Roth C.; Ramaker D. E. Kinetics of CO poisoning in simulated reformat and effect of ru island morphology on PtRu fuel cell catalysts as determined by operando X-ray absorption near edge spectroscopy. *J. Phys. Chem. C.*, **2007**, *111*, 11403-11413; (c) Luschinetz T.; Sklarow A.; Gulden J. Degradation effects on PEM fuel cells supplied with hydrogen from a LOHC system. *Appl. Mech. Mater.*, **2016**, *839*, 165-169.

²⁹ Iguchi, M.; Onishi, N.; Himeda, Y.; Kawanami, H.; *ChemPhysChem* **2019**, *20*, 1296-1300.

³⁰ (a) Geiling J.; Steingerger M.; Ortner F.; Seyfried R.; Nuss A.; Uhrig F.; Lange C.; Öchsner R.; Wasserscheid P.; März M.; Preuster P. Combined dynamic operation of PEM fuel cell and continuous dehydrogenation of perhydro-dibenzyltoluene. *Int. J. Hydrogen Energy*, **2021**, *46*, 35662-35677; (b) Parekh, A. Recent developments of proton exchange membranes for PEMFC: A review. *Front. Energy Res.* 10:956132.

³¹ Naumann, S.; Buchmeiser, M. R.; Latent and Delayed Action Polymerization Systems. *Macromol. Rapid Commun.* **2014**, *35*, 682-701

³² (a) Monsaert. Stijn.; Lozano, A.; Drozdak R.; Van Der Voort, P; Verpoort, F.; Latent olefin metathesis catalysts. *Chem. Soc. Rev.* **2009**, *38*, 3360-3372; (b) Leitgeb, A.; Abbas, M.; Fischer, R. C.; Poater, A.; Cavallo, L.; Slugovc, C. A latent ruthenium based olefin metathesis catalyst with a sterically demanding NHC ligand. *Catal. Sci. Technol.* **2012**, *2*, 1640-1643; (c) Kabro, A.;

Roisnel, T.; Fischmeister, C.; Bruneau, C. Ruthenium–indenylidene olefin metathesis catalyst with enhanced thermal stability. *Chem. Eur. J.* **2010**, *16*, 12255-12261.

³³ Li, J.; Yang, Y., Di, H.; Wang J. Cascade Hydrogenation–Cyclization of Levulinic Acid into γ -Valerolactone Catalyzed by Half-Sandwich Iridium Complexes: A Mechanistic Insight from Density Functional Theory. *J. Org. Chem.* **2021**, *86*, 674-682.